

3D PCDM Probabilistic Shaping Transmission Scheme Based on Chaotic Constellation Mapping

Mengjie Wu, Bo Liu , Jianxin Ren , Yu Bai, Zeqian Guo, Shuyu Zhou, Yilan Ma, Gengyin Chen, Yongyi Yu, Xiangyu Wu , Yaya Mao , Feng Wang, Yongfeng Wu , and Lilong Zhao

Abstract—In this article, a high-security three-dimensional (3D) probabilistic shaping optical transmission system based on prefix-free code distribution matching (PCDM) and Polar code joint coding is proposed. The bit error rate (BER) performance of the communication system is optimized by using the probabilistic shaping effect of PCDM and the strong correction performance of Polar code. Meantime the Logistic and Lorenz chaotic models are used to mask the constellation map for multiple times to ensure the security transmission of data. The experiment verifies the transmission of 28.64Gb/s encrypted PCDM encoded signals on 2km 7-core fiber. At a BER is 1×10^{-3} , the encrypted PCDM encoded signals improve the BER performance about 3dB compared to the conventional unencrypted 3D 32QAM signals. In terms of security performance, the key space of the proposed encryption scheme is up to 10^{119} , and the BER of the illegal receiver is more than 0.4. The experimental results show that the proposed chaotic optical transmission scheme based on the joint encoding of PCDM and Polar can effectively improve the BER and security performance, which is a promising optical communication transmission scheme.

Index Terms—Chaos security, PCDM, system polar coding.

I. INTRODUCTION

WITH the rapid development of optical fiber communication technology, large-capacity optical communication networks are widely used in the Internet of Things, smart city, financial private network and other fields. However, the growth rate of optical network transmission capacity has slowed down and it is difficult to meet the increasing demand for bandwidth [1], [2].

Manuscript received 18 April 2023; revised 19 May 2023; accepted 31 May 2023. Date of publication 5 June 2023; date of current version 14 June 2023. The work was supported in part by the National Key Research and Development Program of China under Grant 2020YFB1805801, in part by the National Natural Science Foundation of China under Grants U22B2009, 62225503, 61835005, 62205151, 62275127, 62171227, U2001601, and 61935005, in part by Jiangsu Provincial Key Research and Development Program under Grants BE2022079 and BE2022055-2, in part by the Natural Science Foundation of Jiangsu Higher Education Institutions of China under Grant 22KJB510031, and in part by the Startup Foundation for Introducing Talent of NUIST. (Corresponding author: Bo Liu.)

The authors are with the Institute of Optics and Electronics, Nanjing University of Information Science and Technology, Nanjing 210044, China (e-mail: 2467322517@qq.com; bo@nuist.edu.cn; 003458@nuist.edu.cn; baiyu1993@126.com; 1281199482@qq.com; 2564098462@qq.com; yilanma@163.com; 286101325@qq.com; 2267295106@qq.com; 1476279183@qq.com; 002807@nuist.edu.cn; 003101@nuist.edu.cn; wuyongfeng@nuist.edu.cn; nk_endy@163.com).

Digital Object Identifier 10.1109/JPHOT.2023.3283030

In order to further improve the transmission capacity of optical network, many advanced coding modulation technologies have been proposed, for example, high-order quadrature amplitude modulation (QAM), probabilistic constellation shaping (PCS) technology, advanced forward error correction (FEC), and multiplexing technology. Among them, PCS is one of the main means to approach Shannon limit. It has received a lot of attention because it can expand channel transmission capacity while maintaining low system complexity [3], [4], [5]. The probabilistic shaping (PS) based coding modulation technology can optimize the probability distribution of uniformly modulated constellations by improving the probability of low energy symbols and reducing the probability of high energy symbols. It can obtain flexible spectral efficiency, enhance the robustness, and effectively improve the transmission performance of optical fiber communication system. As one of the core components of PS, the distribution matcher can convert the information symbol of the uniform probability distribution into the encoded symbol of the target non-uniform probability distribution [6]. At present, the proposed algorithms to realize PS include: constant composition distribution matching (CCDM) [7], enumerated sphere shaping (ESS) [8], prefix-free code distribution matching (PCDM) [9], etc. As the most commonly used fixed-length input-output DM, CCDM has the disadvantage of high operational complexity and it is difficult to implement in parallel application-specific integrated circuit (ASIC) implementations. As an algorithm with high computational efficiency and good shaping gain, PCDM has the advantages of good parallelism and low delay [10]. Its codebook is designed by Huffman code tree and can realize PS flexibly, so it has attracted wide attention.

In the actual transmission of fiber channel, there are several factors may lead error propagation problem when decoding at the receiving end, such as noise, fiber loss and so on. The probabilistic shaping architecture effectively combine PS and FEC encoding to avoid the error propagation problem at the receiving end caused by coding before shaping the sender [11]. Meanwhile, the effect of FEC coding and PS together is better than the performance when they are used separately. In [12], the combination of PCDM and low-density parity check code (LDPC) [13] was proposed to verify the combination of FEC and PS system can effectively improve the BER performance of the transmission system. As a new type of FEC, polar code has low decoding complexity and can approach Shannon limit

theoretically. Its core idea is channel polarization, through channel union and splitting to polarize the channel. When the code length increases indefinitely, part of the channel tends to be noiseless and highly reliable, and part tends to be a purely noisy frozen channel [14]. Experimental results show that Polar code combined with list-cyclic redundancy parity code (CRC) has better performance than LDPC code in the case of short code length [15], [16], [17].

At the same time, the offensive and defensive technologies of optical communication technology are always fighting with each other, and various interception technologies emerge endlessly. However, traditional cryptography [18] based encryption techniques such as Caesar cipher, substitution cipher and DES are no longer applicable to the current complex and diverse data information. The physical layer encryption method based on chaotic encryption provides more methods and means for information encryption. Chaotic models have advantages of high randomness, large iteration space and extreme sensitivity to initial value conditions [19]. While physical layer encryption method based on chaotic model has low cost, low power consumption and high unpredictability, is very suitable for contemporary communication encryption. In recent years, the research on chaotic encryption is also one of the hot spots in the field of optical communication. In [20], the implementation of physical layer encryption using a logistic model is proposed. In [21] Mohamad F. Haroun et al. use the phase information of chaos in the spectrum to modify OFDM symbols to effectively achieve anti-eavesdropping. In [22], Jiang et al. propose a private chaotic phase scrambling technique to effectively encrypt WDM signals into noise-like signals. However, the encryption of optical network transmission system is mainly focuses on the scrambled symbols and carrier frequencies. In this article, a Logistic chaotic model and Lorenz chaotic model are used to implement the joint perturbation of encoding modulation process and constellation symbols, and the original 3D 16QAM constellation map is safely masked into a completely new spherical constellation map. Moreover, a set of PCDM codebooks are designed for the data transmission and used jointly with Polar codes, resulting in improved BER performance of the encrypted data.

In order to meet the requirements of communication capacity and security performance in current optical network, we propose a 3D PCDM probabilistic shaping transmission scheme based on chaotic constellation mapping. In the process of PS of original data by PCDM, Polar code suppresses the error propagation during the decoding of the receiver and improves the BER performance of transmission system. At the same time, Logistic and Lorenz chaotic models were used to generate masking vectors to rotate the constellation map for several times, and the key space reaches 10^{119} . In the experiment, the PCDM signals and the conventional 3D-32QAM signals were respectively transmitted at 28.64 Gb/s. At a BER is 1×10^{-3} , the sensitivity of the PCDM signal is about 3 dB higher than the conventional 3D-32QAM signals. It shows that the proposed security transmission system has not only high security performance but also good BER performance.

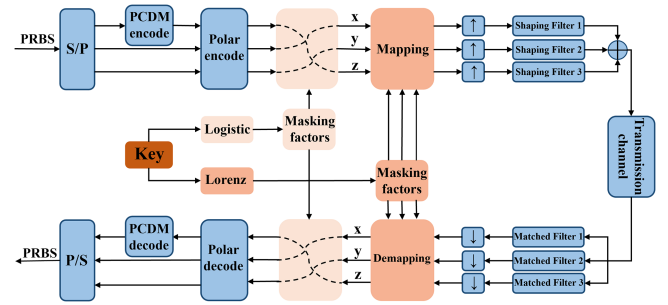


Fig. 1. Schematic diagram of a high-security 3D constellation shaping transmission scheme based on PCDM coding.

II. PRINCIPLES

Fig. 1 depicts the principle of a high-security 3D constellation shaping transmission scheme based on PCDM coding. The input pseudo-random binary sequences (PRBS) are converted into three channels by series to parallel (S/P) converting. One of them is sent into the PCDM encoder and Polar encoder, and the other are encoded by Polar encoder directly. The PCDM converts the uniformly distributed binary sequence into the unipolar amplitude symbols of the target probability distribution. The frozen redundant bits generated by Polar coding are used as symbol bits, and then combine unipolar amplitude symbols to get bipolar amplitude symbols. Logistic and Lorenz models are used to generate masking vectors and perform coded modulation process masking and constellation masking, respectively. The key is composed of the initial value and control parameters of the chaotic models. Then, 3D carrier-less amplitude phase (CAP) modulation is used including up-sampling, shaped filtering and addition. Finally, the encrypted symbols are transmitted to a 7-core fiber for transmission.

The codebook of PCDM adopted in this article is implemented by Huffman code. The codebook is designed according to the output symbol of the target probability distribution with the lowest average energy as the optimization criterion. The average energy E_s is obtained by calculating the ratio of the input binary sequence to the output coded symbol of the codebook:

$$E_s = \frac{E(\|X\|^2)}{E(l(X))} = \frac{\sum_{x_i \in X} 2^{-l(\varphi^{-1}(x_i))} \times \|x_i\|^2}{\sum_{x_i \in X} 2^{-l(\varphi^{-1}(x_i))} \times l(x_i)} \quad (1)$$

$$\beta = \frac{E(l(B))}{E(l(X))} = \frac{\sum_{b_i \in B} 2^{-l(b_i)} \times l(b_i)}{\sum_{x_i \in X} 2^{-l(\varphi^{-1}(x_i))} \times l(x_i)} \quad (2)$$

where E_s is the average energy of the output symbols, X is the set of output coded symbols, B is the set of input information symbols, φ^{-1} represents the mapping relationship between the output coding symbol and the input binary sequence, $E()$ represents the mathematical expectation, and $l()$ represents the length of the output symbols. In this scheme, the codebook capacity $C = 11$, the average energy is 3.05, coding rate is 0.751. The specific codebook is shown in Table I, and its corresponding Huffman code tree is shown in Fig. 2. PCDM uses variable-length coding

TABLE I
 CODEBOOK OF PCDM

Input bits	Output Coded Symbols
00	3
01	131
100	11131
101	111113
110	111111
11100	111131
11101	1133
11110	11133
111110	1131
1111110	111133
1111111	133

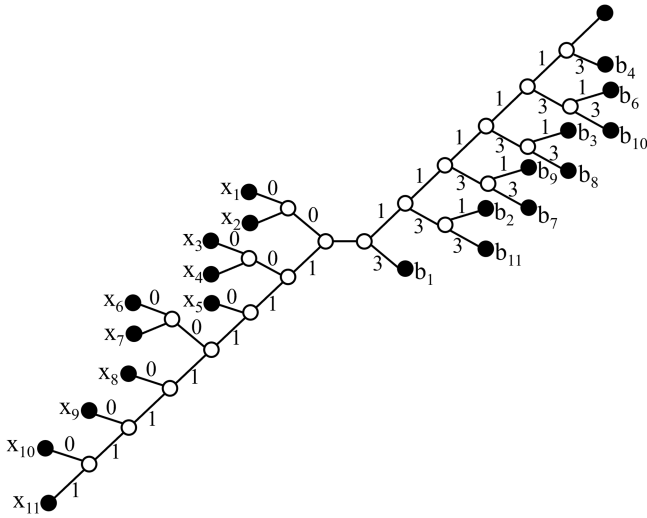


Fig. 2. The Huffman code tree corresponding to Table I.

method, that is, both input bits and output symbols are of variable length. With the target codebook capacity determined, we can change the number and positions of the root and leaf nodes of the left and right binary trees of the Huffman coding tree to obtain the best mapped codebooks with the same E_s and different coding rates β . According to the target coding rate, a set of PCDM codebooks with β value of 0.751 is selected for subsequent experimental study in this article. The Huffman code tree adopted in Fig. 2 is a full binary tree, which can traverse the transmitted data if the code length is sufficient. After PCDM coding, the data changes from the original uniformly distributed 0 and 1 symbols, to unevenly distributed 1 and 3 symbols. As the probability of occurrence of symbol 1 is greater compared to symbol 3, the probability of occurrence of the inner circle constellation points is greater. Thus, probabilistic shaping is achieved. The unipolar amplitude symbols are obtained by Huffman code. Then, the unipolar symbols are encoded by Polar encoder. The step size of the system Polar code is set to 1024, and the code rate is 3/4. The step size of the system

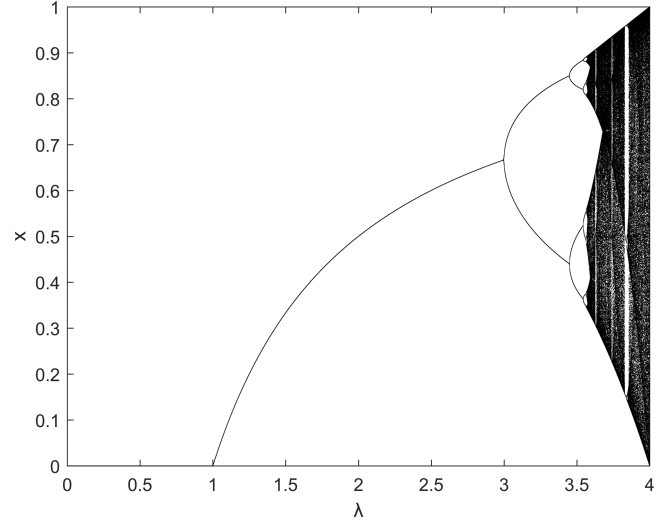


Fig. 3. Bifurcation diagram of the logistic chaos model.

Polar code is set to 1024, and the code rate is 3/4. The method of Gaussian approximation is used here for the construction of polar code to obtain the capacity of different bit channels, and the serial cancellation list (SCL) algorithm is adopted for the Polar decoder. The frozen redundant bits generated by Polar code are reused as symbol bits and combined with the unipolar amplitude symbols to obtain the encoded bipolar symbols for the final data transmission.

For the security of optical network transmission system, two chaotic models, Logistic and Lorenz, are used to carry out coding modulation and constellation symbol joint scrambling. Logistic model is used to encrypt the encoding process for the first time. The mapping model is as follows:

$$\mu_{n+1} = \lambda \mu_n (1 - \mu_n) \quad (3)$$

where $n = 0, 1, 2, \dots$, λ and μ_0 are initial values, respectively set to 3.9 and 0.9. Fig. 3 is the bifurcation diagram of the logistic chaotic model. When $3.5699456 < \lambda \leq 4$, the iterated values of the model are in a pseudo-random state. When the parameter λ is constant, for any initial value μ_0 , the unique sequence will be iterated. Even a small change in the initial value of μ_0 will result in different sequences. Logistic chaotic model shows complex chaotic dynamics behavior and has high security performance. The specific rules for masking vector generation are as follows:

$$M = \text{floor}(\text{mod}(\mu \cdot 10^{17}, 3)) \quad (4)$$

For the given initial value μ_0 , three possible remainder results can be obtained: 0, 1, 2. As an example, suppose that data is transmitted using rule 6, as shown in Table II. After processing (4) of the chaotic sequence, the remainder result sequence is 010120. The number 0 indicates that the data output by PCDM encoder is the z coordinate. The other two are respectively the μ coordinate and y coordinate, thus forming a constellation point (x_1, y_1, z_{p1}) . When the number is 1, the output of PCDM encoded data is y

TABLE II
SELECTIVE MAPPING RULES BASED ON LOGISTIC CHAOS MASKING

Remainder	Coordinate	Rule1	Rule2	Rule3	Rule4	Rule5	Rule6
0	x	x_p	x_p	x'	x'	x'	x'
	y	y'	y'	y_p	y_p	y'	y'
	z	z'	z'	z'	z'	z_p	z_p
1	x	x'	x'	x_p	x'	x_p	x'
	y	y_p	y'	y'	y'	y'	y_p
	z	z'	z_p	z'	z_p	z'	z'
2	x	x'	x'	x'	x_p	x'	x_p
	y	y'	y_p	y'	y'	y_p	y'
	z	z_p	z'	z_p	z'	z'	z'

Then, Lorenz model is used to generate three sets of chaotic

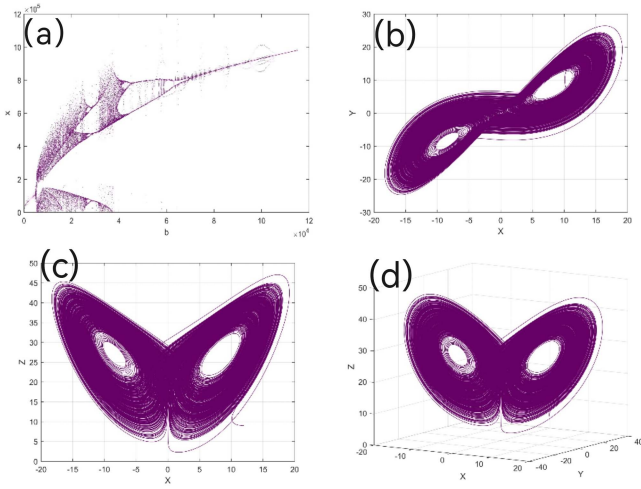


Fig. 4. (a) Bifurcation and (b), (c), (d) phase diagram of the Lorenz model.

coordinate, and the other two are x coordinate and z coordinate respectively, forming constellation points (x_2, y_{p2}, z_2) . Thus, random masking of each constellation point can be achieved. The constellation map after the first constellation masking is shown in Fig. 5(b). After the encryption of the encoding modulation process is completed, the data encoded by PCDM is randomly masked in 3 ways coordinate information. The constellation map is also changed from the original 3D 16QAM to 32QAM.

Then, Lorenz model is used to generate three sets of chaotic vectors at the same time, and constellation scrambling was carried out on 32 constellation points obtained after the first masking. The Lorenz model is expressed as follows:

$$\begin{cases} \frac{dx}{dt} = a(y - x) \\ \frac{dy}{dt} = x(b - z) - y \\ \frac{dz}{dt} = xy - cz \end{cases} \quad (5)$$

where t is the step size, a , b and c are constants, respectively set as: 10, 28 and 2.667, x , y and z are the chaotic sequences generated by this model. Lorenz model has complex chaotic dynamics behavior and pseudo-randomness. Its bifurcation and

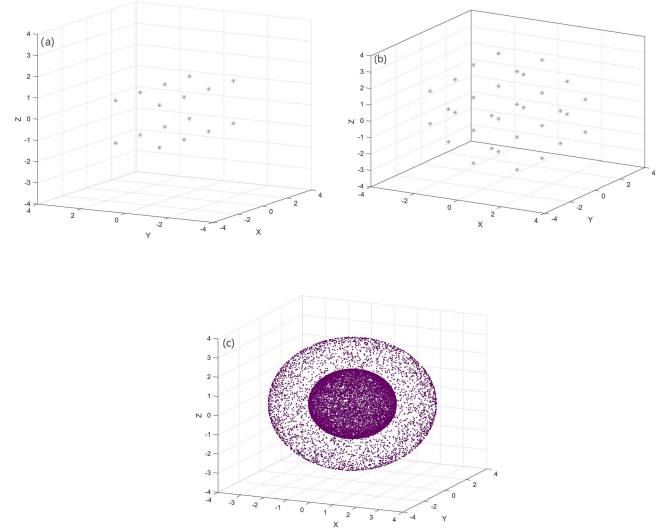


Fig. 5. (a) Original unencrypted constellation map; (b) the constellation map after the first encryption; (c) the constellation map after the second encryption.

phase diagrams are shown in Fig. 4. When the value of b is greater than 25, the system gradually approaches the chaotic state. We set the initial value of this model to $(x', y', z') = (12, 29)$. As shown in the Fig. 4, $x \in (-20, 20)$, $y \in (-20, 20)$, $z \in (0, 50)$. The 3D Lorenz chaotic model can simultaneously generate three independent sets of chaotic sequences (x, y, z) , and use the decimal part of the chaotic sequences to generate masking factor. The masking factor is processed by Formula (6), and the rotation angle of the constellation point will be limited in $(0, 360^\circ)$. The $\omega_1, \omega_2, \omega_3$ are the rotation angle of the inner counterclockwise rotation about the axes x, y, z , respectively.

$$\begin{cases} \omega_1 = \text{floor}(\text{mod}(x \cdot 10^7, 360)) \\ \omega_2 = \text{floor}(\text{mod}(y \cdot 10^7, 360)) \\ \omega_3 = \text{floor}(\text{mod}(z \cdot 10^7, 360)) \end{cases} \quad (6)$$

Set the coordinates of any constellation point are $R_i = (r_1, r_2, r_3)^T$, then the coordinates after chaotic masking can be expressed as:

$$R'_i = (r_1, r_2, r_3)^T = \begin{pmatrix} \cos \omega_3 & -\sin \omega_3 & 0 \\ \sin \omega_3 & \cos \omega_3 & 0 \\ 0 & 0 & 1 \end{pmatrix} \begin{pmatrix} \cos \omega_2 & 0 & -\sin \omega_2 \\ 0 & 1 & 0 \\ \sin \omega_2 & 0 & \cos \omega_2 \end{pmatrix} \cdot \begin{pmatrix} 1 & 0 & 0 \\ 0 & \cos \omega_1 & -\sin \omega_1 \\ 0 & \sin \omega_1 & \cos \omega_1 \end{pmatrix} \cdot R_i \quad (7)$$

where R'_i is the coordinates of the constellation points after rotating around the x, y, z axes respectively. Fig. 5(c) shows the constellation map after being masked by the constellation twice. By rotating and encrypting the constellation points twice, the illegal receiver can hardly restore the original data information

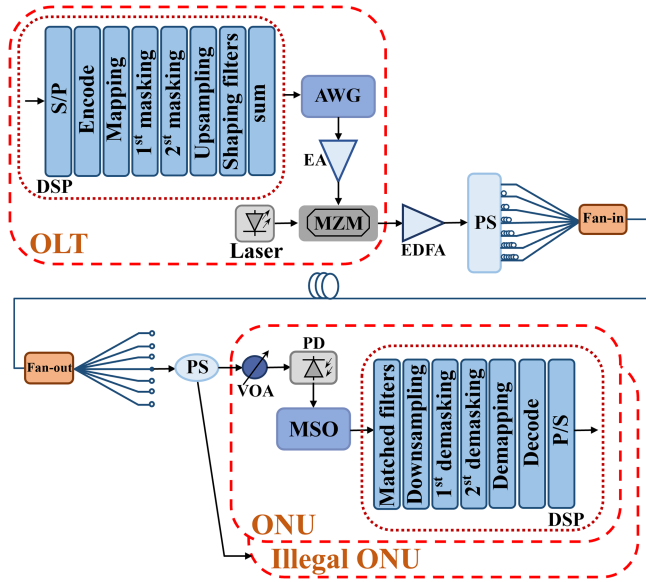


Fig. 6. Experimental setup (AWG: arbitrary waveform generator; EA: electrical amplifier; MZM: Mach-Zehnder modulator; EDFA: Erbium-doped fiber amplifier; PS: power splitter; VOA: variable optical attenuator; PD: photodiode; MSO: mixed signal oscilloscope).

according to the constellation points without knowing the key. Thus, the security of data transmission is ensured after PCDM and Polar joint coding.

III. EXPERIMENTAL SETUP AND RESULTS

In order to verify the performance of the proposed encrypted transmission system based on the joint encoding of PCDM and Polar, an experiment is carried out as shown in Fig. 6. The transmission is carried out by 2 km 7-core single-mode optical fiber. It has a low attenuation characteristic, and the attenuation coefficient is less than 0.3 dB/km at 1550 nm wavelength. In addition, each core uses a fan-in fan-out device, which allows negligible insertion loss while ensuring accurate core spacing and connection points. The encrypted data is generated by offline digital signal processing (DSP) at the sending end, and the encrypted data is modulated by a three-dimensional CAP with an up-sampling factor of 11. The experimental light source is a continuous wavelength laser with a working wavelength of 1550 nm and power of 10 dBm. The arbitrary waveform generator (AWG, TekAWG70002A) performs digital-to-analog conversion of encrypted PCDM signals at a sampling rate of 15 GSa/s. After the signal is modulated by an electrical amplifier (EA), it is sent to a Mach-Zehnder modulator (MZM) for intensity modulation. Then the signal is amplified by an Erbium-doped fiber amplifier (EDFA) and fanned into a 2 km 7-core fiber after passing through a power splitter (PS). At the receiving optical network unit (ONU), the received optical power is first adjusted by a variable optical attenuator (VOA), and then the converted optical signal is detected by a photodiode (PD). Then the electrical signal is sampled with a mixed signal oscilloscope (Tektronix, MSO73304DX) with a

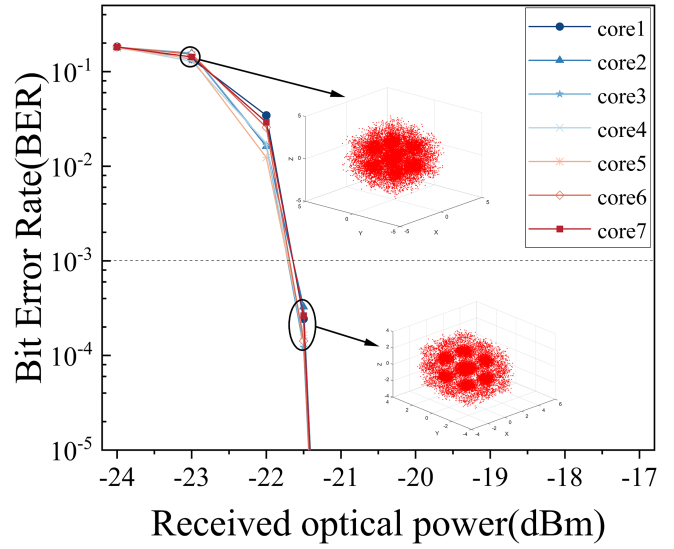


Fig. 7. BER performance at different optical powers in a 7-core fiber after 2 km transmission.

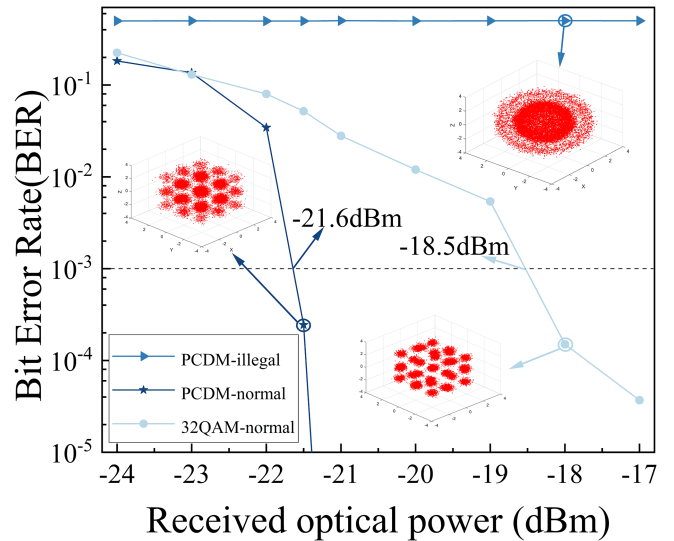


Fig. 8. BER curves of PCDM signals and 3D-32QAM signals.

sampling rate of 50Gs/s. Finally, the corresponding decryption work is carried out on the offline DSP to recover the original data.

Fig. 7 shows the BER curve of 2 km transmission of encrypted PCDM signal in 7-core fibers. It can be seen that the BER of 7 cores decreases obviously with the increase of optical power at the legal ONU. At a BER of 1×10^{-3} , the receiving sensitivity of the best core is about 0.08 dB higher than the worst core. The BER curves of the 7 cores almost coincide, indicating that the performance of the 7-core single-mode fiber is stable and isolation between the cores is good.

Fig. 8 depicts the BER performance curves of PCDM signals at legal ONU and illegal ONU. To fairly compare the BER performance, the AWG sampling rate are set as 9 GSa/s and

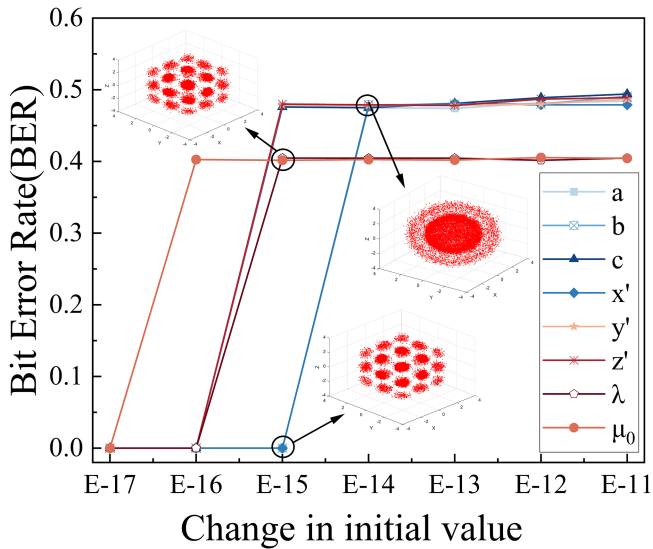


Fig. 9. BER curves of ONUs with a tiny change in initial value.

15 GSa/s respectively. As far as the signal is concerned, the net bit rate can be tantamount to the expression of (AWG sampling rate \times entropy)/ up-sampling factor. So transmitted in a 7-core fiber, the net bit rate of 3D-32QAM signals and PCDM signals, are same 28.64Gb/s (4.09Gb/s \times 7). It can be seen from the Fig. 8, as the optical power increases, the BER performance of PCDM signals and conventional 3D-32QAM signals shows a downward trend. At a BER of 1×10^{-3} , the BER performance of PCDM signals are about 3dB higher than that of conventional 3D-32QAM signals. This is attributed to the PS effect of PCDM, and the strong error correction ability of Polar code restrains the error propagation and synchronization error to some extent. At the illegal receiver, the BER of the received PCDM signals are about 0.5. As can be seen from Fig. 8, the constellation diagram of the illegal receiver is completely unsolved, indicating that, it is almost impossible for the eavesdrop to crack the information and recover the correct constellation diagram without the key of the encryption system. The results show that the proposed high security 3D constellation shaping transmission scheme based on the joint encoding of PCDM and Polar can ensure the security transmission of data.

Furthermore, the key space size of this transmission scheme is analyzed. The keys of this transmission scheme mainly include the initial values and control parameters of Logistic and Lorenz chaotic models, namely (a, b, c, x' , y' , z' , λ , μ_0) is (10, 28, 2.667, 12, 2, 9, 3.9, 0.9). In order to explore the sensitivity of the key, we test the BER performance when each parameter of the key changes slightly. The experimental received optical power is -17 dBm, as shown in Fig. 9, where the x-coordinate represents the accuracy of the changed parameter. Taking z' and μ_0 as examples. when the value of parameter z' changes greater than 10^{-16} , the BER increases significantly until about 0.5, the illegal ONUs are completely unable to eavesdrop on data. However, since these two parameters belong to different chaotic

models, they have different sensitivities to initial values and different contributions to BER performance, the worst BER is almost 0.4. Although the constellation map is correct, the BER is still very high, and the illegal receivers still cannot obtain the correct data information. The size of the conservative key space is $(1 \times 10^{15}) \times (1 \times 10^{14}) \times (1 \times 10^{15}) \times (1 \times 10^{14}) \times (1 \times 10^{15}) \times (1 \times 10^{15}) \times (1 \times 10^{15}) \times (1 \times 10^{16}) = 10^{119}$. The key space is large enough to resist brute force attacks by illegal receivers.

IV. CONCLUSION

In this article, a probabilistic shaping code modulation scheme based on PCDM is proposed. The flexible PCDM probabilistic shaping and Polar code are combined to improve the transmission performance of 3D PS communication system. Different chaotic models are used to mask the probabilistic shaping modulation process and constellation mapping multiple times. The security of the communication system is improved. The encrypted PCDM signal with a transmission rate of 28.64 Gb/s is verified by experiments on 2 km 7-core fiber. With a BER of 1×10^{-3} , the encrypted PCDM signals improve the BER performance by about 3dB compared with the conventional unencrypted 3D-32QAM signals. In terms of security performance, the BER of the information obtained by the illegal receiver is more than 0.4. The key space of the proposed encryption scheme is 10^{119} , and large enough to ensure the security performance of the communication system. Experimental results show that the proposed chaotic security optical transmission scheme based on the joint encoding of PCDM and Polar can effectively improve the BER and security performance, which is a promising optical communication transmission scheme.

REFERENCES

- [1] K. - I. Kitayama, A. Maruta, and Y. Yoshida, "Digital coherent technology for optical fiber and radio-over-fiber transmission systems," *J. Lightw. Technol.*, vol. 32, no. 20, pp. 3411–3420, Oct. 2014.
- [2] L. J. Zhang, B. Liu, X. Xin, Q. Zhang, J. Yu, and Y. Wang, "Theory and performance analyses in secure CO-OFDM transmission system based on two-dimensional permutation," *J. Lightw. Technol.*, vol. 31, no. 1, pp. 74–80, Jan. 2013.
- [3] J. X. Ren et al., "A probabilistically shaped star-CAP-16/32 modulation based on constellation design with honeycomb-like decision regions," *Opt. Exp.*, vol. 27, no. 3, pp. 2732–2746, Feb. 2019.
- [4] J. Y. Shi et al., "Improved performance of high-order QAM OFDM based on probabilistically shaping in the datacom," in *Proc. Opt. Fiber Commun. Conf. Expo.*, 2018, pp. 1–3.
- [5] C. P. Pan and F. R. Kschischang, "Probabilistic 16-QAM shaping in WDM systems," *J. Lightw. Technol.*, vol. 34, no. 18, pp. 4285–4292, Sep. 2016.
- [6] J. H. Cho, "Prefix-free code distribution matching for probabilistic constellation shaping," *IEEE Trans. Commun.*, vol. 68, no. 2, pp. 670–682, Feb. 2020.
- [7] P. Schulte and G. Böcherer, "Constant composition distribution matching," *IEEE Trans. Inf. Theory*, vol. 62, no. 1, pp. 430–434, Jan. 2016.
- [8] A. Amari et al., "Introducing enumerative sphere shaping for optical communication systems with short blocklengths," *J. Lightw. Technol.*, vol. 37, no. 23, pp. 5926–5936, Dec. 2019.
- [9] J. H. Cho et al., "Prefix-free code distribution matching for 5G new radio," 2020, *arXiv:2001.05810*.

- [10] Q. Y. Yu, S. Corteselli, and J. Cho, "FPGA implementation of rate-adaptable prefix-free code distribution matching for probabilistic constellation shaping," *J. Lightw. Technol.*, vol. 39, no. 4, pp. 1072–1080, Feb. 2021.
- [11] J. H. Cho and P. J. Winzer, "Probabilistic constellation shaping for optical fiber communications," *J. Lightw. Technol.*, vol. 37, no. 6, pp. 1590–1607, Mar. 2019.
- [12] H. Li et al., "LDPC-coded 50-Gbaud IM/DD PAM-4 transmission employing probabilistic amplitude shaping based on prefix-free code distribution matching," *Opt. Fiber Technol.*, vol. 66, Oct. 2021, Art. no. 102670.
- [13] R. Gallager, "Low-density parity-check codes," *IRE Trans. Inf. Theory*, vol. 8, no. 1, pp. 21–28, Jan. 1962.
- [14] E. Arikan, "Channel polarization: A method for constructing capacity-achieving codes for symmetric binary-input memoryless channels," *IEEE Trans. Inf. Theory*, vol. 55, no. 7, pp. 3051–3073, Jul. 2009.
- [15] T. Koike-Akino et al., "Bit-interleaved polar-coded modulation for low-latency short-block transmission," in *Proc. Opt. Fiber Commun. Conf. Exhib.*, 2017, pp. 1–3.
- [16] Y. Zuo et al., "Performance analysis of polar code with SCL algorithm in ultraviolet communication system," in *Proc. Asia Commun. Photon. Conf. Int. Conf. Inf. Photon. Opt. Commun.*, 2020, pp. 1–3.
- [17] H. H. Zhou et al., "Polar coded probabilistic shaping PAM8 based on many-to-one mapping for short-reach optical interconnection," *Opt. Exp.*, vol. 29, no. 7, pp. 10209–10220, Mar. 2021.
- [18] H. G. Situ et al., "Double random-phase encoding in the Fresnel domain," *Opt. Lett.*, vol. 29, no. 14, pp. 1584–1586, 2004.
- [19] R. Tang et al., "High security OFDM-PON based on an iterative cascading chaotic model and 4-D joint encryption," *Opt. Commun.*, vol. 495, Sep. 2021, Art. no. 127055.
- [20] J. Y. Zhao et al., "High-security physical layer in CAP-PON system based on floating probability disturbance," *IEEE Photon. Technol. Lett.*, vol. 32, no. 7, pp. 367–370, Apr. 2020.
- [21] M. F. Haroun et al., "Secure OFDM with peak-to-average power ratio reduction using the spectral phase of chaotic signals," *Entropy*, vol. 23, no. 11, Nov. 2021, Art. no. 1380.
- [22] A. K. Zhao, N. Jiang, S. Liu, Y. Zhang, and K. Qiu, "Physical layer encryption for WDM optical communication systems using private chaotic phase scrambling," *J. Lightw. Technol.*, vol. 39, no. 8, pp. 2288–2295, Apr. 2021.